

Numerical Analysis on IVR-ERVC using Lagrangian CFD – Modeling & Preliminary Results

Tae Hoon Lee^a, So Hyun Park^a, Hoon Chae^a, Yeon-Gun Lee^b Eung Soo Kim^{a*}

^aDepartment of Nuclear Engineering, Seoul National University, 1 Gwank-ro, Gwanak-gu, Seoul, South Korea

^bDepartment of Nuclear and Energy Engineering, Jeju National University, 102 Jejudaehak-ro, Jeju-si, Jeju 63243

*Corresponding author: kes7741@snu.ac.kr

1. Introduction

In-Vessel Retention through External Reactor Vessel Cooling (IVR-ERVC) is a severe accident management strategy for early termination. The key of the IVR-ERVC strategy is to ensure the integrity of reactor vessel by stably and continuously removing the thermal load out of the molten core through external cooling [1]. In this study, a numerical analysis has been conducted to understand the transient behavior in the IVR-ERVC, which involves various complex physical and chemical phenomena including natural circulation, stratification, thermal ablation, crust formation, radiation, conjugate heat transfer, and etc. In order to capture the phenomena, the molten core behavior in the reactor vessel was modeled using a smoothed particle hydrodynamic (SPH) method, which is a well-known meshless computational fluid dynamic (CFD). On the other hand, the external vessel cooling governed by two-phase natural circulation was modeled using the MARS-KS code, a 1-D system code.

2. Methodology

The SOPHIA code is a GPU-based multi-physics code developed for addressing safety-related phenomena in the nuclear reactors [2]. This code is based on the numerical method called smoothed particle hydrodynamics (SPH), which is one of the most well-known Lagrangian meshless CFD. In this method, fluid is represented by an aggregate of finite particles, and the properties (mass, velocity, temperature, etc.) of the particles is determined according to the type of fluid and the particle spacing. After setting initial conditions for the particles, the phenomenon is calculated through interaction between the central particle and the surrounding particles [3].

In this study, the SOPHIA code was used for modeling the molten core behaviors in the reactor vessel. The governing equations in the SPH discretization are summarized in Table 1. In this modeling, mass, momentum, and energy conservations were solved with an equation of state (EOS). The standard k-ε model was used for considering turbulence effect and Non-Boussinesq model was used for handling natural convection. Thermal ablation and crust formation were modeled using a simple phase-change model, in which the material phase (solid/liquid) is switched depending on the thermodynamic conditions.

Table 1. The governing equation applied to SOPHIA code

Mass conservation	
$\left(\frac{\rho}{\rho_{ref}}\right)_i = \sum_j \frac{m_j}{\rho_{ref,j}} W_{ij}$	(3)
Momentum conservation	
$\left(\frac{du}{dt}\right)_i = \left(\frac{du}{dt}\right)_i^{fp} + \left(\frac{du}{dt}\right)_i^{fv} + \mathbf{g} + f_{ext}$	(4)
$\left(\frac{du}{dt}\right)_i^{fp} = -\sum_j m_j \left(\frac{p_i+p_j}{\rho_i\rho_j}\right) \nabla W_{ij}$	(5)
$\left(\frac{du}{dt}\right)_i^{fv} = \sum_j \frac{4m_j}{\rho_i\rho_j} \frac{\mu_i\mu_j}{(\mu_i+\mu_j)} (\mathbf{u}_i - \mathbf{u}_j) \frac{r_{ij}\cdot\nabla W_{ij}}{(r_{ij} ^2+\eta^2)}$	(6)
Turbulence model	
$\left(\frac{dk}{dt}\right)_i = P_i - \epsilon_i + \sum_j \frac{4m_j}{\rho_i\rho_j} \frac{\mu_{k,i}\mu_{k,j}}{(\mu_{k,i}+\mu_{k,j})} k_{ij} \frac{r_{ij}\cdot\nabla W_{ij}}{ r_{ij} ^2}$	(7)
$\left(\frac{d\epsilon}{dt}\right)_i = \frac{\epsilon_i}{k_i} (C_{\epsilon,1}P_i - C_{\epsilon,2}\epsilon_i) + \sum_j \frac{4m_j}{\rho_i\rho_j} \frac{\mu_{\epsilon,i}\mu_{\epsilon,j}}{(\mu_{\epsilon,i}+\mu_{\epsilon,j})} \epsilon_{ij} \frac{r_{ij}\cdot\nabla W_{ij}}{ r_{ij} ^2}$	(8)
$\mu_{k,\epsilon} = \mu_v + \frac{\mu_T}{\sigma_{k,\epsilon}} \quad \mu_T = \frac{\rho C_\mu k^2}{\epsilon}$	
$P_i = \min(P_{k,i}, \sqrt{C_\mu k_i S_i}) \quad P_{k,i} = \frac{C_\mu k_i^2 S_i^2}{\epsilon_i}$	
$S_i = -\frac{1}{2} \sum_j m_j \frac{\rho_i+\rho_j}{\rho_i\rho_j} \mathbf{u}_i - \mathbf{u}_j ^2 \frac{r_{ij}\cdot\nabla W_{ij}}{(r_{ij} ^2+\eta^2)}$	
Energy conservation	
$\left(\frac{dh}{dt}\right)_i = \sum_j \frac{4m_j}{\rho_i\rho_j} \frac{k_i k_j}{(k_i+k_j)} (T_i - T_j) \frac{r_{ij}\cdot\nabla W_{ij}}{(r_{ij} ^2+\eta^2)} + \dot{q}_i$	(9)
Equation of State	
$p = \frac{c_0^2 \rho_{ref,i}}{\gamma} \left[\left(\frac{\rho}{\rho_{ref,i}} \right)^\gamma - 1 \right]$	(10)
Non-Boussinesq model	
$\rho_{ref,i} = \rho_{0,i} (1 - \alpha_T (T_i - T_{ref,i}))$	(11)
$m_i = \rho_{ref,i} \cdot V_{0,i}$	(12)

In this study, a MARS-KS code was used for analysis of external vessel cooling by two-phase water natural circulation. The SOPHIA-MARS coupling is performed through socket programming. In this coupling, the vessel wall heat flux and temperature were exchanged between the SOPHIA code and the MARS-KS code at every timestep.

In this study, APR-1400 reactor was selected for the benchmark analysis. The simulation setup and conditions were selected by referring to the progress of the accident

in the previous study of the Korea Atomic Energy Research Institute [4]. It is composed of a molten metal pool and a molten oxide pool of different densities, and decay heat is generated in the molten oxide pool. Cooling is performed through a reactor vessel wall, and cooling is performed by radiative heat transfer in the upper part of the molten metal pool.

During the accident process of previous studies, 35,000 seconds were judged as the severest interpretation condition, and the analysis was performed by setting this time as the initial condition. The shape of the lower head of the reactor is shown in Fig. 1, and the analysis conditions are shown in Table 2. The simulation was performed in a 1/4 hemispherical shape for the efficiency of calculation, and the analysis shape was supplemented by applying a symmetric boundary.

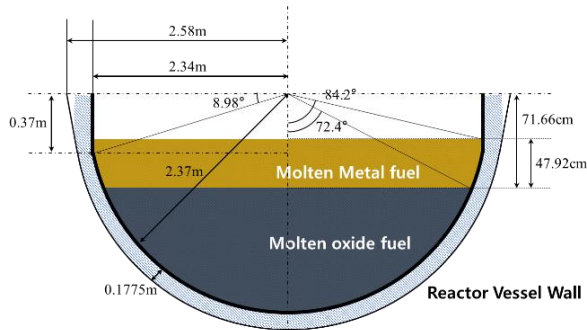


Fig. 1. IVR-ERVC Geometry and Configuration

Table 2. Simulation parameter and conditions

Parameter	Value	
Oxide corium	Density (kg/m^3)	8191
	Dynamic viscosity ($\text{Pa}\cdot\text{s}$)	4.7×10^{-3}
	Thermal exp. coeff. (K^{-1})	1.0×10^{-3}
	Conductivity ($\text{W/m}\cdot\text{K}$)	5.3
	Specific heat ($\text{J/kg}\cdot\text{K}$)	533.2
	Initial Temperature (K)	4009.3
Metal corium	Density (kg/m^3)	6899.2
	Dynamic viscosity ($\text{Pa}\cdot\text{s}$)	4.0×10^{-3}
	Thermal exp. coeff. (K^{-1})	1.0×10^{-3}
	Conductivity ($\text{W/m}\cdot\text{K}$)	25
	Specific heat ($\text{J/kg}\cdot\text{K}$)	789.5
	Initial Temperature (K)	4041.86
Volumetric heating power (W/m^3)	1.25×10^6	
Rayleigh number (Ra)	1.65×10^{17}	
Prandtl number (Pr)	0.473	

3. Results and Discussions

Fig. 2 shows the overall situations and the temperature distribution of the molten core pool during the IVR-ERVC condition qualitatively. In this figure, the molten metal pool and the molten oxide pool are stratified stably and exhibit individual natural circulation. The molten

metal pool forms a flow based on the fact that heat is transferred from the molten oxide pool at the lower part, radiative heat transfer on the upper surface, and cooling is performed through interaction with the external wall. The molten oxide pool is heated by internal decay heat and cooled by an external vessel wall. At the top, a constant temperature distribution appears due to mixing by convective flow. At the lower part, a stratified temperature distribution appears, and at the bottom, crust formed by solidification is stacked. The external vessel wall ablation by melt through interaction is observed at the metal layer. The oxide crust formation is also observed at the bottom part of the reactor internal vessel.

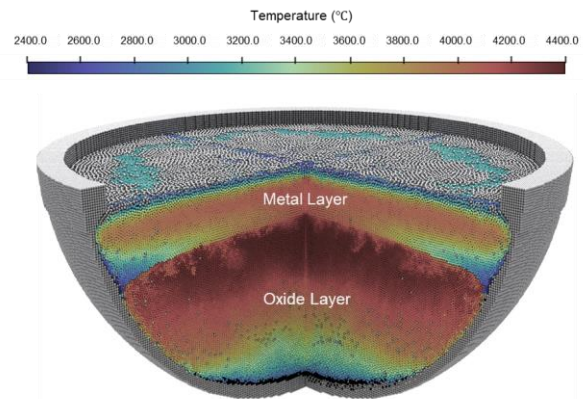


Fig. 2. Snapshot of IVR-ERVC simulation

In this study, quantitative analysis was conducted by comparisons with the previous study conducted by lumped parameter codes. Fig. 3 compares the heat flux distribution at the reactor vessel wall. According to this result, the present study over-predicts the heat flux at the bottom while it under-predicts the value at the top in comparisons with the LPM codes. The main reason is still not well clarified yet, but it seems to be due to the heat conduction effect along the thick metallic vessel wall. Ablation and crust-formation are also considered to be other reasons.

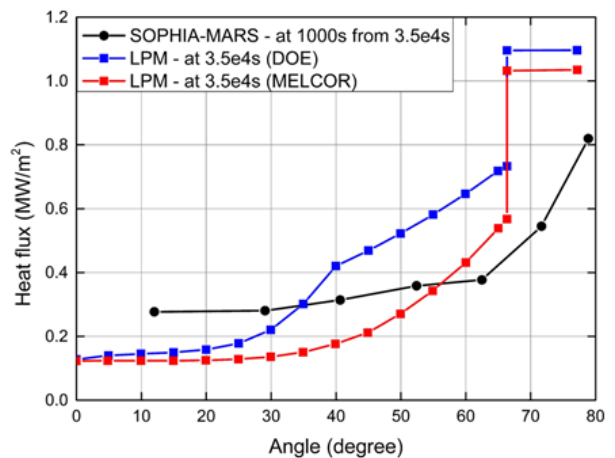


Fig. 3. Heat flux distribution on reactor vessel wall

4. Conclusions

In this study, the IVR-ERVC strategy was numerically analyzed for APR-1400 reactor conditions through the SOPHIA-MARS integrated analysis code. Complex molten core behaviors such as natural convection, heat transfer, stratification, turbulence, thermal ablation by melting and crust formation by solidification were calculated using the SOPHIA code. The external cooling system and the two-phase natural convection flow were calculated using the MARS-KS code. An integrated analysis code was constructed through the Socket program, and the calculation was performed by exchanging heat flux and temperature. The simulation performance results were compared with the LPM calculation in previous studies, and qualitative comparisons were performed due to differences in initial conditions and assumptions. The distribution of heat flux was compared according to the angle, and the tendency was consistent with previous study. However, there were somewhat discrepancies in the detailed values and further investigations are needed to clarify it.

ACKNOWLEDGEMENT

This work was supported by the National Research Foundation of Korea (NRF) grant funded by the Korea government (MSIT). (No. 2021M2D2A1A03046881)

This work was supported by the Nuclear Safety Research Program through the Korea Foundation Of Nuclear Safety(KoFONS) using the financial resource granted by the Nuclear Safety and Security Commission(NSSC) of the Republic of Korea. (No. 2103079)

REFERENCES

- [1] Ma, W., Yuan, Y., & Sehgal, B. R. (2016). In-vessel melt retention of pressurized water reactors: historical review and future research needs. *Engineering*, 2(1), 103-111.
- [2] Jo, Y. B., Park, S. H., Choi, H. Y., Jung, H. W., Kim, Y. J., & Kim, E. S. (2019). SOPHIA: Development of Lagrangianbased CFD code for nuclear thermal-hydraulics and safety applications. *Annals of Nuclear Energy*, 124, 132-149.
- [3] Monaghan, J. J. (2005). Smoothed particle hydrodynamics. *Reports on progress in physics*, 68(8), 1703.
- [4] Lim, K., Cho, Y., Whang, S., & Park, H. S. (2017). Evaluation of an IVR-ERVC strategy for a high power reactor using MELCOR 2.1. *Annals of Nuclear Energy*, 109, 337-349.